# Electronic Supplementary Information

## Ligand Engineering of Immobilized Nanoclusters on Surfaces: Ligand Exchange Reactions with Supported $Au_{11}(PPh_3)_7Br_3$

*Vera Truttmann,[a] Christopher Herzig,[b] Ivonne Illes,[b] Andreas Limbeck,[b] Ernst Pittenauer,[b] Michael Stöger-Pollach,[c] Günter Allmaier,[b] Thomas Bürgi,[d] Noelia Barrabés *[a] and Günther Rupprechter [a]*

[a] Institute of Materials Chemistry, Technische Universität Wien, Getreidemarkt 9/165, 1060 Vienna, Austria
[b] Institute of Chemical Technologies and Analytics, Technische Universität Wien, Getreidemarkt 9/164, 1060 Vienna, Austria
[c] University Service Center for Transmission Electron Microscopy (USTEM), Technische Universität Wien, Wiedner Hauptstraße 8-10, 1040 Vienna, Austria
[d] Department of Physical Chemistry, University of Geneva, Quai Ernest Ansermet 30, 1211 Geneva, Switzerland

### Experimental Section

**Chemicals.** Hydrogen tetrachloroaurate (III) trihydrate ($HAuCl_4 \cdot 3\ H_2O$, 99,99%, Alfa Aesar), Tetraoctylammonium bromide (TOAB, ≥98%, Alfa Aesar), Triphenylphosphine ($PPh_3$, >95%, Sigma Aldrich), Sodium borohydride ($NaBH_4$, 98%, Alfa Aesar), L-Glutathione reduced (GSH, ≥99%, Sigma Aldrich), 2-Phenylethanethiol (2-PET, 98%, Sigma Aldrich), L-Glutathione oxidized (GSSG, ≥98%, Lactan), Fluorescein Isothiocyanate (FITC, ≥90%, Lactan), tris(2-carboxyethyl)phosphine hydrochloride (TCEP, TCI Chemicals), 5,5'-dithiobis(2-nitrobenzoic acid) (DTNB, ≥99%, Lactan), *trans*-2-[3-(4-*tert*-Butylphenyl)-2-methyl-2-propenylidene]malononitrile (DCTB, ≥99%, Sigma Aldrich), 2',4',6'-Trihydroxyacetophenone Monohydrate (THAP, ≥99,5%, Sigma Aldrich), 40% Acrylamide/Bis-acrylamide solution 19:1 (99,9%, Bio-Rad), 2-Amino-2-(hydroxymethyl)-1,3-propanediol (Tris base, ≥99,8%, Bio-Rad), glycine (Bio-Rad), Ammonium persulfate (APS, Bio-Rad), *N*,*N*,*N'*,*N'*-Tetramethylethylenediamine (TEMED, Bio-Rad). Acetonitrile, chloroform, DCM, DMF, glacial acetic acid, glycerol, hexane, methanol, THF and toluene were obtained from commercial suppliers. Milli-Q water (18.2 MΩ) was used for all procedures. Reagents from commercial suppliers were used without further purification. If the purity of the chemicals could not be ensured, they were distilled (liquids) or recrystallized (solids) prior to use.

**Synthesis of $Au_{11}(PPh_3)_7Br_3$ Nanoclusters.** The synthesis of $Au_{11}(PPh_3)_7Br_3$ was carried out based on previously published protocols.[1-5] $HAuCl_4 \cdot 3\ H_2O$ (1 eq., 500 mg, 1.27 mmol) and TOAB (1.2 eq., 833 mg, 1.52 mmol) were dissolved in THF (50 ml), giving a clear orange solution. Upon addition of $PPh_3$ (5 eq., 1165 mg, 6.35 mmol), the color faded out within a few minutes. After stirring at room temperature for one hour, $NaBH_4$ (10 eq., 480 mg, 12.70 mmol) dissolved in ice-cold $H_2O$ (10 ml) was added at once. The solution was kept stirring at high speed under ambient conditions for 48 hours, resulting in the formation of a reddish-brown precipitate. Afterwards, the solvent was removed under reduced pressure at room temperature, and the remaining solid repeatedly washed with 1:1 MeOH:$H_2O$. This was followed by extraction of by-products with THF, toluene and 2:1 hexane:EtOH. The process was followed by UV-Vis, with the by-products showing a prominent absorption band at 411 nm. The $Au_{11}(PPh_3)_7Br_3$ cluster was then extracted with DCM, again followed by UV-Vis. The cluster showed prominent bands at 383 and 422 nm. Evaporation of the solvent gave $Au_{11}(PPh_3)_7Br_3$ as an orange powder. Yield: 195 mg (40%). $^1$H NMR ($\delta$, $CD_2Cl_2$, 20 °C): 7.38 (br m, 2H, $H_{ortho}$), 6.89 (t, $J$ = 7.2 Hz, 1H, $H_{para}$), 6.60 (dd, $J_1 = J_2$ = 7.6 Hz, 2H, $H_{meta}$). $^{31}$P NMR ($\delta$, $CD_2Cl_2$, 20 °C): 52.8. UV-Vis ($CH_2Cl_2$, nm): 293 (shoulder), 309, 383, 422, 515 (shoulder). MALDI-MS (DCTB, $CH_2Cl_2$): 4161 $[Au_{11}(PPh_3)_7Br_2]^+$.

**Synthesis of the F-GSH ligand.** The synthesis of the Fluorescein-labeled glutathione (F-GSH) was carried out following a procedure reported by Landino and coworkers.[6] Small adjustments were made in the reduction step, when the pH value of the aqueous solution was adjusted with 10 N KOH to 7.4 instead of using a buffer when adding tris(2-carboxyethyl)phosphine hydrochloride (TCEP) (to a concentration of 50 mM). Completion of the reduction to F-GSH was indicated by formation of a yellow-orange precipitate (around 30 minutes to 2 hours when stirred at room temperature). Complete reduction was confirmed by TLC ($R_f$ value 0.34 with acetonitrile/water/glacial acetic acid (80:20:1) as mobile phase). Separation and purification was then performed using C8 or C18 solid phase extraction columns and washing with water until no excess TCEP could be detected anymore (free TCEP gives a yellow solution when mixed with a 10 mM solution of 5,5'-dithiobis(2-nitrobenzoic acid) (DTNB) in 0,1 M phosphate buffer at pH 7.4). The final product F-GSH was then eluted with methanol, the solvent removed under reduced pressure and the yellow-orange powder stored under a $N_2$ atmosphere. UV-Vis (MeOH, nm): 370, 425 (shoulder), 455, 480. Photoluminescence (MeOH, nm): 520, 545, 603 (shoulder).

**Ligand Exchange with GSH in solution to $Au_{25}(SG)_{18}$.** The ligand exchange was conducted according to literature.[1] An excess of GSH (10 eq., 56 mg, 0.18 mmol) in 10 ml of Milli-Q water was added to a solution of $Au_{11}(PPh_3)_7Br_3$ (1 eq., 10 mg, 0.0024 mmol) dissolved in 10 ml of $CHCl_3$. The reaction mixture was stirred rapidly for 6 hours at 50 °C under nitrogen atmosphere. Afterwards, phases were separated and the colored aqueous phase washed several times with $CHCl_3$. After evaporation of the solvent, $Au_{25}(SG)_{18}$ was yielded as a brown solid. Purification of the product was achieved by polyacrylamide gel electrophoresis (PAGE). UV-Vis ($CH_2Cl_2$, nm): 410, 455, 505 (shoulder), 670.

**Ligand Exchange with 2-PET in solution to $[Au_{25}(PPh_3)_{10}(SC_2H_4Ph)_5Br_2]^{2+}$.** The reaction was conducted according to literature procedures.[7-11] For a typical ligand exchange reaction, a solution of $Au_{11}(PPh_3)_7Br_3$ (1 eq., 14.7 mg, 0.0036 mmol) dissolved in 15 ml of $CHCl_3$ was heated up to 50 °C and an excess of 2-PET was added (75 eq., 36 µl, 0.27 mmol). The reaction was conducted for 24 hours under reflux. After evaporation of the solvent, the residue was washed three times with hexane to remove free ligands. $[Au_{25}(PPh_3)_{10}(SC_2H_4Ph)_5Br_2]^{2+}$ was yielded as a green solid in high purity. UV-Vis ($CH_2Cl_2$, nm): 315, 328 (shoulder), 368 (shoulder), 415, 445 (shoulder), 520 (weak shoulder), 680.

**Ligand Exchange with GSH on an $Al_2O_3$ surface.** A solution of $Au_{11}(PPh_3)_7Br_3$ (1 eq., 2.5 mg, 0.61 µmol) in 1-2 ml of DCM was dropcasted onto a polished $Al_2O_3$ surface (on an aluminum plate). Prior to use, the plates were polished with Metadi Diamond Polishing Compound (1 and ¼ micron, Buehler) and rinsed with EtOH. After evaporation of the solvent, the sample was placed in a solution of GSH (160 eq., 30 mg, 0.098 mmol) in 10 ml $H_2O$:MeOH (8:2). After 3 days at room temperature, the plate was taken out and rinsed with 8:2 $H_2O$:MeOH and small amounts of MeOH to remove excess ligands. PM-IRRAS spectra were recorded of $Au_{11}(PPh_3)_7Br_3$ in the beginning, during the reaction and of the final product, referred to as [$Au_{11}$:GSH] in the following. For MALDI measurements of [$Au_{11}$:GSH], a small amount of sample was scratched off the plate and dissolved in MeOH.

**Ligand Exchange with F-GSH on an $Al_2O_3$ surface.** The reaction was carried in the same way as the ligand exchange with GSH on an $Al_2O_3$ surface described in the last paragraph. A solution of $Au_{11}(PPh_3)_7Br_3$ (1 eq., 2.5 mg, 0.61 µmol) in 1-2 ml of DCM was dropcasted onto a polished $Al_2O_3$ surface (of an aluminum plate). Prior to use, the plates were polished with Metadi Diamond Polishing Compound (1 and ¼ micron, Buehler) and rinsed with EtOH. After evaporation of the solvent, the sample was placed in a solution of F-GSH (160 eq., 68 mg, 0.098 mmol) in 10 ml $H_2O$:MeOH (8:2). After 1 day at room temperature, the plate was taken out and rinsed with 8:2 $H_2O$:MeOH and small amounts of MeOH to remove excess ligands. The product is referred to as [$Au_{11}$:F-GSH] in the following.

**Ligand Exchange with GSH on a ZnSe crystal.** A solution of $Au_{11}(PPh_3)_7Br_3$ (1 eq., 5 mg, 1.2 µmol) in 1-2 ml of EtOH was dropcasted onto a ZnSe ATR crystal. After evaporation of the solvent, the crystal was positioned in the flow cell. A 0.01 M solution of GSH in 8:2 $H_2O$:MeOH was pumped through the cell at 0.05 ml/min over a period of 30 hours, allowing *in-situ* ATR-IR monitoring of the reaction. The solution was then removed and the product [$Au_{11}$:GSH] rinsed with 8:2 $H_2O$:MeOH and small amounts of MeOH to remove excess ligands. Spectra of the dry dropcast films of $Au_{11}(PPh_3)_7Br_3$, [$Au_{11}$:GSH] and the exchange ligand GSH were also recorded.

**Ligand Exchange with 2-PET on an $Al_2O_3$ surface.** A solution of $Au_{11}(PPh_3)_7Br_3$ (1 eq., 3 mg, 0.73 µmol) in 1-2 ml of DCM was dropcasted onto a polished $Al_2O_3$ surface (on an aluminum plate). Prior to use, the plates were polished with Metadi Diamond Polishing Compound (1 and ¼ micron, Buehler) and rinsed with EtOH. After evaporation of the solvent, the sample was placed in a solution of 2-PET (200 eq., 20 µl, 0.15 mmol) in 10 ml of toluene. After one day at room temperature, the plate was taken out and rinsed with hexane and small amounts of DCM to remove excess ligands. A new solution of 2-PET (200 eq., 20 µl, 0.15 mmol) in 10 ml of 8:2 toluene:$CHCl_3$ was prepared and the sample placed therein for another day. It was then again rinsed with hexane and DCM and then placed in a solution of 2-PET (200 eq., 20 µl, 0.15 mmol) in 10 ml of 7:3 toluene:$CHCl_3$ for additional 2 days. Afterwards, it was washed with hexane and DCM for a final time. PM-IRRAS spectra were recorded of $Au_{11}(PPh_3)_7Br_3$ in the beginning, between the changes of the solvents and of the final product, referred to as [$Au_{11}$:2-PET] in the following. For MALDI measurements of [$Au_{11}$:2-PET], a small amount of sample was scratched off the plate and dissolved in MeOH.

The same experiment was also carried out using hexane instead of toluene as the main solvent, yielding a product [$Au_{11}$:2-PET]'.

**Characterizations Techniques**

**UV-Vis** spectra of the clusters were recorded on either a PerkinElmer 750 Lambda or a Varian Cary 50 Bio spectrometer at room temperature, using quartz glass cuvettes with 1 cm path length. Depending on the nature of the sample, different solvents (DCM, THF, $H_2O$) were used. Measurements with solid samples were performed using a PerkinElmer 750 Lambda spectrometer with an integrating sphere with an inner diameter of 60 mm. The spectra were recorded in diffuse transmittance mode, using cuvettes with 0.5 or 1 cm path length.

**Photoluminescence** spectroscopy was conducted employing an Edinburgh FSP920 photoluminescence spectrometer equipped with a XE900 Xenon arc lamp, Czerny-Turner monochromators TMS300 and a S900 photomultiplier R928 detector. A step size of 2 nm and 0.25 s dwell time were used. Both dissolved samples in different solvents (DCM, MeOH, $H_2O$) in quartz glass cuvettes (90° geometry) and supported analytes on the aluminum sample plates were measured. Emission scans with a fixed excitation at 400 nm (solution, solid state) or at 450 nm (solid state) were recorded. When recording spectra of analytes in solution, a 455 nm cut-off filter was inserted after the sample to prevent that second order diffraction radiation was reaching the detector.

**MALDI** mass spectra were measured using either a prototype Axima MALDI $ToF^2$ time of flight (TOF) MS (Shimadzu, Kratos Analytical) or a Bruker Autoflex mass spectrometer. The spectra were obtained working at near threshold laser irradiances of the nitrogen laser in positive linear mode. Averaging 300-600 spectra of single laser pulses (λ = 337 nm at 50 Hz) obtained by rastering over the sample gave the spectra displayed within this publication. Depending on the samples, different matrixes (DCTB or THAP), solvents (DCM, $CHCl_3$, MeOH) and analyte:matrix ratios (between 1:10 and 1:100) were used.

**Nuclear magnetic resonance (NMR)** spectra were recorded on a Bruker Avance-250 spectrometer at 250 MHz ($^1H$) or at 101.20 MHz ($^{31}P$). The chemical shift is reported in parts per million from tetramethylsilane ($^1H$) or 85% phorphoric acid ($^{31}P$). $CDCl_3$ was used as solvent.

**Polyacrylamide gel electrophoresis (PAGE)** was performed on a Bio-Rad Protean II xi cell holding one or two 1.5x16x16 cm slab gels. The separation and extraction procedure was conducted according to published protocols,[12, 13] with only slight differences. The gels were prepared native without SDS, with 30 wt% and 3 wt% monomer (acrylamide:bisacrylamide = 19:1) in separating and stacking gel, respectively. The samples were dissolved in 1:1 $H_2O$/glycerol mixture and loaded into the wells of the stacking gel. A 1.92 M glycine and 250 mM tris base eluting buffer was used. The electrophoresis was run at constant voltage (150 V) for 6 hours. Afterwards, the gel pieces containing clusters were crushed and extracted in 4 °C cold water for 1 day. The gel residue was then removed by filtration and 2% acetic acid was added. The solution was then concentrated under reduced pressure and the clusters precipitated by addition of 1.5 ml of methanol and centrifugation. After redissolving in 600 µl of $H_2O$, the precipitation and centrifugation were repeated twice with smaller volumes (1 ml and 0.75 ml) of methanol, to achieve higher purity.

**ATR-IR** was measured on a Bruker Vertex 70 FTIR spectrometer with a liquid nitrogen cooled MCT detector. A specac flow cell was used for the ligand exchange reaction, through which the solution of GSH in 8:2 $H_2O$/MeOH was flown at low speed (0.05 ml/min). The sample was dropcasted on a ZnSe

crystal (52(48) mm x 20 mm x 2 mm) with EtOH or $H_2O$. All spectra were recorded at room temperature.

**PM-IRRAS** spectra were recorded on a Bruker Tensor 27 FT-IR spectrometer, with the external beam port being connected to a Bruker PMA 50 unit. A photoelastic modulator PEM 90 (Hinds) at 50 Hz was used for modulation; demodulation of the signal was achieved with a Stanford Research SR830 DSP lock-in amplifier. The spectrometer was equipped with a MCT detector, which was cooled with liquid nitrogen. Samples were mounted on an IRRAS sample holder and measurements were done at an angle of incidence of 80°. All spectra were recorded at room temperature, using a high pass filter with a cut-off at 3800 $cm^{-1}$. The samples were dropcasted centrally on small planar aluminum plates (see above) and the plates were dried for at least 5 hours before measuring. The same position on the plate was chosen for all measurements.

**Transmission electron microscopic (TEM)** and high-angle annular dark-field scanning electron microscopic (HAADF-STEM) images were obtained at the University Service Center for Transmission Electron Microscopy (USTEM) of TU Wien. A FEI Tecnai F20 S-TWIN analytical (scanning) transmission electron microscopy [(S)TEM] instrument at an accelerating voltage of 200 kV was used. An energy resolution of approximately 1 eV and a spatial resolution of approximately 0.5 nm could be achieved. The sample was dispersed in a small amount of $CH_2Cl_2$ and one drop placed on a carbon film-covered TEM copper grid.

**LA-ICP-MS** measurements were performed using a commercially available laser ablation system (New Wave 213, ESI, Fremont, CA) with a frequency quintupled 213 nm Nd:YAG laser in combination with a quadrupole ICP-MS instrument (Thermo iCAP Qc, ThermoFisher Scientific, Bremen, Germany). The instrument was tuned for maximum $^{115}In$ signal using NIST612 (National Institute of Standards and Technology, Gaithersburg, MD). The samples dropcasted onto aluminum substrates were ablated in line mode. Four lines with 17 mm length were applied on each sample for ICP-MS analysis. Further details on measurement parameters are given in Table S1. With these ablation parameters it can be ensured that the Au complex is ablated completely, though sample thickness varies along the scan route due to sample preparation method.

For signal quantification a dried droplet approach combined with micro grooves is applied and intensity ratios are used for quantification[14, 15]. Therefore liquid single standards of P, S (Specpure®, Alfa Aesar, ThermoFisher, Germany) are pairwise mixed with an Au (BDH Prolabo ®, VWR Chemicals, Belgum) single standard. For each analyte/Au pair, a separate calibration based on mass ratios is prepared. All further quantification is likewise based on the intensity ratio of each analyte respectively and the $^{197}Au$ signal. The calibration ranged from 0.01 – 0.20 µg analyte/µg Au. Microgrooves were produced on aluminum substrates by using the laser ablation system. For each calibration solution four lines with 5 mm length, 0.4 mm distance in between, 100 µm spot size and 5.5 $J/cm^2$ were ablated. These microgrooves are filled with the liquid standard mixtures, the solvent evaporates and the remaining residue is ablated with the same instrument parameters as the samples.
The transient signal, achieved by ablation of the samples or standards, was divided into several subsections. Of each subsection (region) an intensity ratio was formed. 24 of such ratios for one single analyte (6 regions for one line, 4 lines/sample) were averaged and regression curves could be obtained thereby. Within the calibration range correlation coefficients (COD) of $r^2 = 0.98$ for P/Au and $r^2 = 0.96$ for S/Au were calculated.

**Table S1:** Instrumentation and measurement parameters; *Parameters for preparation of microgrooves

| Laser ablation system | NWR213, New Wave Research | ICP-MS | iCAP Q, Thermo Scientific |
|---|---|---|---|
| Type of laser | Nd:YAG 213 nm | RF power [W] | 1450 |
| Ablation mode | Lines | Carrier gas flow rate [L $min^{-1}$] | 0.6 |
| Beam diameter [µm] | 100* / 150 | Plasma gas flow rate [L $min^{-1}$] | 14 |
| Fluence [J $cm^{-2}$] | 5.5* / 3.3 | Auxiliary gas flow rate [L $min^{-1}$] | 0.8 |
| Frequency [Hz] | 20 | Acquisition time [ms] | 10 |
| Scan speed [µm $s^{-1}$] | 150 | Cones | Ni |
| He gas flow [L $min^{-1}$] | 0.65 | Measured isotopes | $^{31}P$, $^{32}S$, $^{197}Au$ |

For the investigation of the dropcasted samples, intensities ratios P/Au and S/Au of $Au_{11}(PPh_3)_7Br_3$, [$Au_{11}$:GSH] and [$Au_{11}$:2-PET] were calculated by integrating the signals of repetitive measurements in 3 areas. This compensates for varying sample thicknesses over the length of the cluster dropcasts. The process is demonstrated graphically in Figure S1 for the Au signal of one measurement of [$Au_{11}$:GSH].

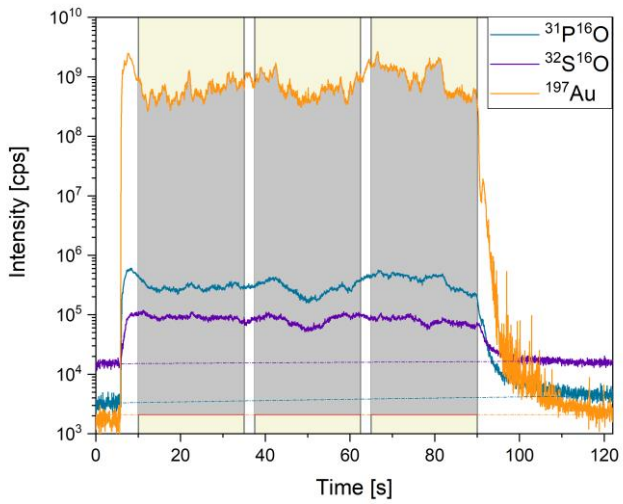


**Figure S1:** Integration windows for the LA-ICP-MS measurements shown for the Au signal of [$Au_{11}$:GSH].

## Ligand exchange reactions of $Au_{11}(PPh_3)_7Br_3$ with Thiolates in solution

### Ligand exchange with GSH in solution to $Au_{25}(SG)_{18}$

The exchange reaction was followed with UV-Vis and MALDI-MS. The decrease of the characteristic bands of $Au_{11}(PPh_3)_7Br_3$ in the organic layer over the course of the reaction is clearly visible in the UV-Vis spectra in Figure S2. The absorption in the $H_2O$ phase intensified during the ligand exchange, with the characteristic bands of $Au_{25}(SG)_{18}$ appearing at 410, 455 and 670 nm. Purification by PAGE then yielded $Au_{25}(SG)_{18}$ in high purity.

When looking at the MALDI mass spectra of the $CHCl_3$ phase (Figure S3) recorded over the progress of the reaction, the vanishing of $Au_{11}(PPh_3)_7Br_3$ is clearly visible and most prominent in the first 4 hours of reaction. Afterwards, only smaller fragments are observed in the organic phase, which might be related to decomposed clusters.
Complimentary MALDI mass spectra of the aqueous phase containing the main product $Au_{25}(SG)_{18}$ could not be acquired at the instruments available.

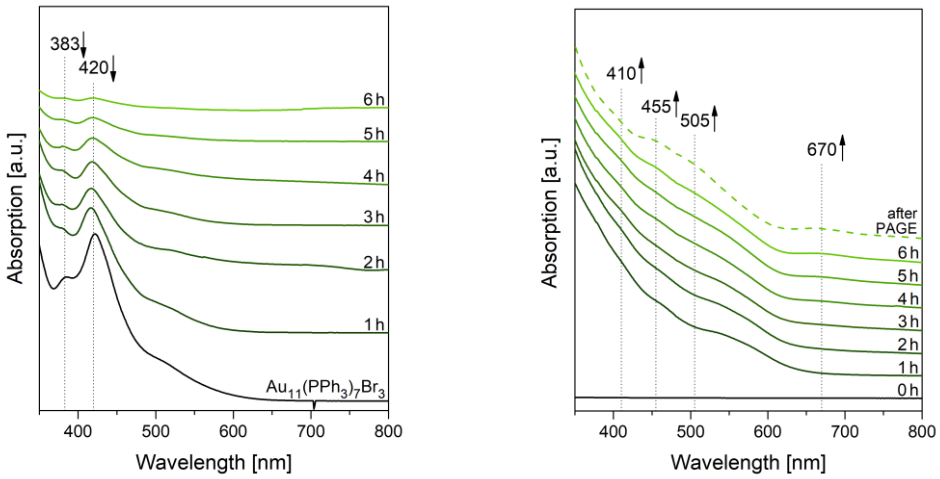


**Figure S2**: UV-Vis spectra of the ligand exchange of $Au_{11}(PPh_3)_7Br_3$ with GSH in solution to $Au_{25}(SG)_{18}$: $CHCl_3$ (left) and $H_2O$ phase (right)

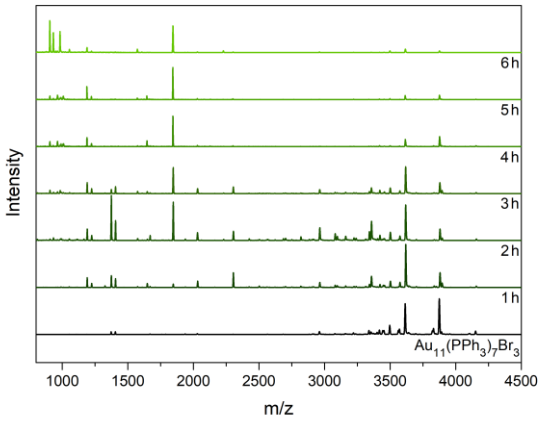


**Figure S3**: MALDI mass spectra of the $CHCl_3$ phase of the ligand exchange of $Au_{11}(PPh_3)_7Br_3$ with GSH in solution to $Au_{25}(SG)_{18}$

**Ligand exchange with 2-PET in solution to $[Au_{25}(PPh_3)_{10}(SC_2H_4Ph)_5Br_2]^{2+}$**

The exchange reaction was followed with UV-Vis and MALDI-MS. In UV-Vis (Figure S4), the formation of the most characteristic bands of $[Au_{25}(PPh_3)_{10}(SC_2H_4Ph)_5Br_2]^{2+}$ at ≈445 $cm^{-1}$ and ≈680 $cm^{-1}$ can be observed even after only 15 minutes. This indicates quite rapid exchange. After 24 hours, the spectrum clearly resembles that of $[Au_{25}(PPh_3)_{10}(SC_2H_4Ph)_5Br_2]^{2+}$.

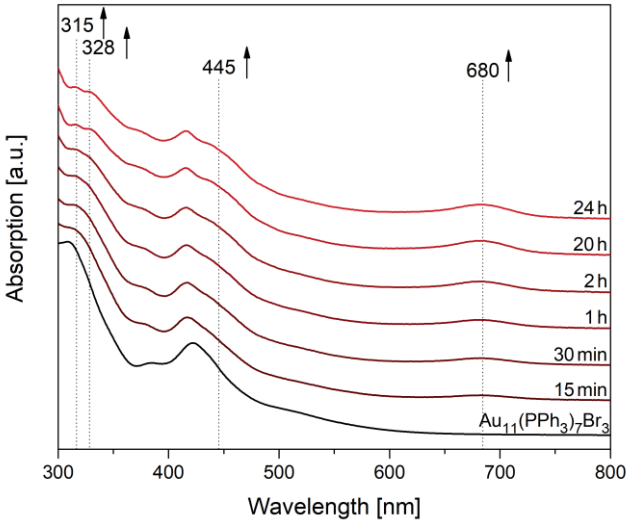


**Figure S4**: UV-Vis spectra of the ligand exchange of $Au_{11}(PPh_3)_7Br_3$ with 2-PET in solution to $[Au_{25}(PPh_3)_{10}(SC_2H_4Ph)_5Br_2]^{2+}$

The same trend is observed by MALDI-MS in Figure S5. After only 15 minutes, the clusters have already started to grow, resulting in a polydisperse mixture. With progressing reaction, a size-focusing process occurs, which yields very pure $[Au_{25}(PPh_3)_{10}(SC_2H_4Ph)_5Br_2]^{2+}$ after 24 hours.

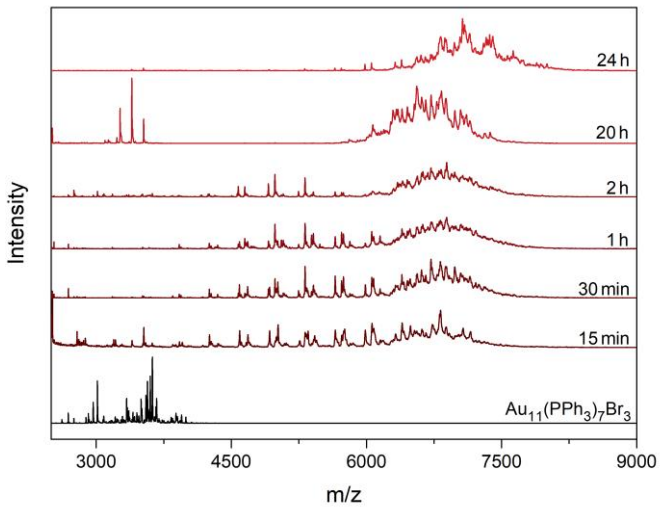


**Figure S5**: MALDI mass spectra of the ligand exchange of $Au_{11}(PPh_3)_7Br_3$ with 2-PET in solution to $[Au_{25}(PPh_3)_{10}(SC_2H_4Ph)_5Br_2]^{2+}$

**Additional MALDI-MS spectrum of $Au_{11}(PPh_3)_7Br_3$, [$Au_{11}$:GSH] and [$Au_{11}$:2-PET]**

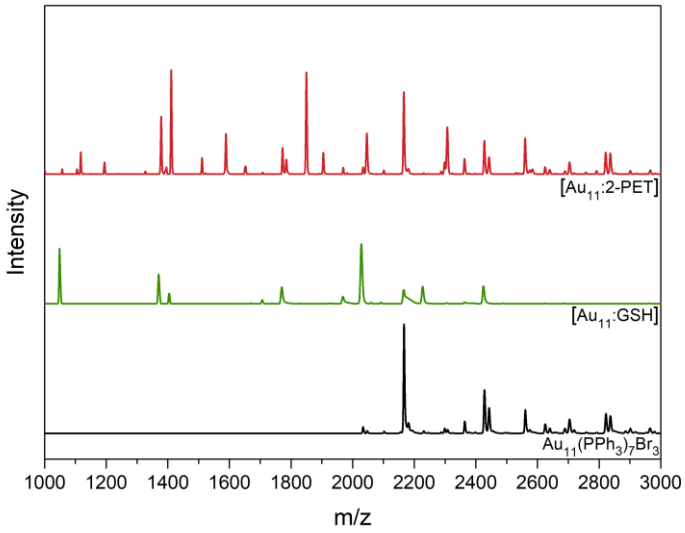


**Figure S6**: MALDI-MS spectra of $Au_{11}(PPh_3)_7Br_3$, [$Au_{11}$:GSH] and [$Au_{11}$:2-PET] at lower m/z

**Additional LA-ICP-MS measurements**

Blank experiments were conducted by placing polished support plates in the solutions containing the thiol ligands, GSH and 2-PET, respectively. The plates were kept in solution for 48 hours and afterwards rinsed with pure solvent to remove excess ligands (alike conducting the real experiment). Afterwards, LA-ICP-MS measurements were carried out. As can be seen in Figure S7, the signals of these blank experiments are significantly smaller compared to those obtained of the exchanged samples, [$Au_{11}$:GSH] and [$Au_{11}$:2-PET]. Thus, binding of the thiol ligands to the support surface can be neglected within this study and free thiol ligands remaining on the plate after the exchange experiment were removed in the subsequent washing steps.

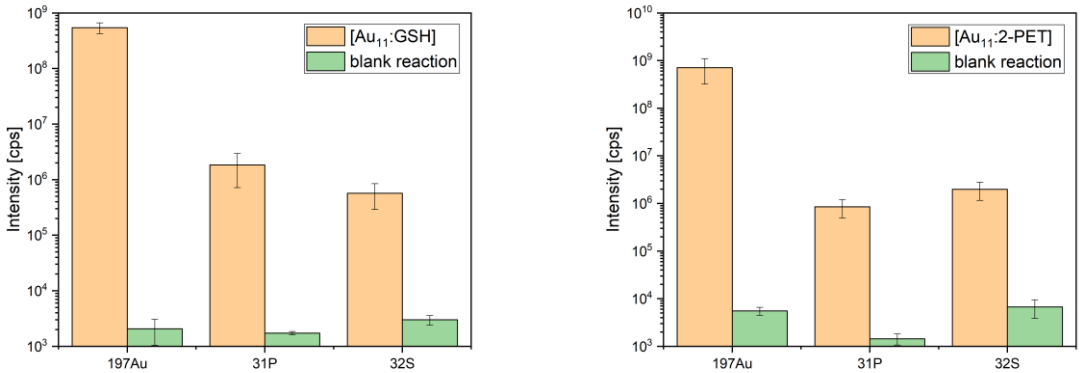


**Figure S7:** Comparison of the LA-ICP-MS intensities of the ligand exchange experiments with (orange) and without (green) cluster dropcast on the plate surface: (left) GSH exchange; (right) 2-PET exchange.

In addition, as leaching of the clusters was indicated by a slight color change of the solution of the [$Au_{11}$:2-PET] system, LA-ICP-MS measurements of the solution before and after the reaction were obtained (Figure S8). An increase of the $^{197}Au$ signal was noted, confirming the assumed leaching to the solution. In addition, also an increase in the $^{31}P$ signal could be found, which indicates dissolution of ligand protected Au units. However, further assessment would be required to determine their exact composition.

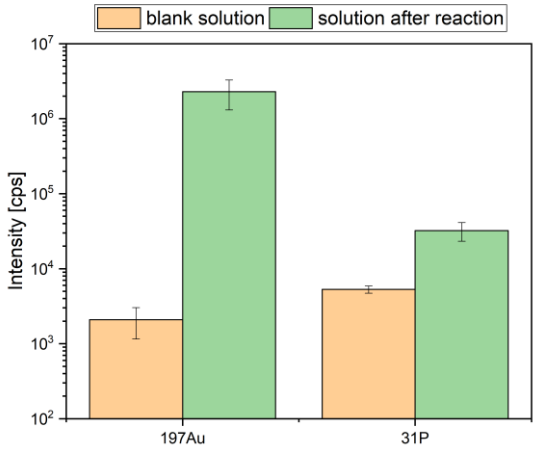


**Figure S8:** Comparison of the LA-ICP-MS intensities of the reaction solution of the [$Au_{11}$:2-PET] system: before (orange) and after the reaction (green).

**(S)TEM images of $Au_{11}$, [$Au_{11}$:GSH], [$Au_{11}$:GSH] and $Au_{25}$ nanoclusters**

To further ensure the stability of the clusters upon exposure to excess thiols, the reacted products [$Au_{11}$:GSH] and [$Au_{11}$:2-PET] were investigated with TEM (Figure S9a and Figure S9b). Similar to MALDI-MS, a small amount of dropcast sample was scratched off the support plate, dissolved in DCM and dropcasted onto a copper grid for microscopy. The distribution was found to be very uniform, with a particle size of ≈1 nm. Similar values were reported for supported $Au_{11}$ before,[16] and could also be observed for the pure starting cluster $Au_{11}(PPh_3)_7Br_3$. HAADF-STEM (Figure S9c) was chosen in this case, due to strong charging effects in TEM mode. To further confirm the different reactivities of $Au_{11}$ in solution and on a surface, HAADF-STEM images of $Au_{25}(SC_2H_4Ph)_{18}^-$ were obtained (Figure S9d). They showed clearly identifiable isolated clusters of ≈1.2 nm size, which is significantly larger than $Au_{11}$. This provides further evidence for the stability of the $Au_{11}$ nanoclusters under the conditions of the ligand exchange, with no $Au_{25}$ being formed.

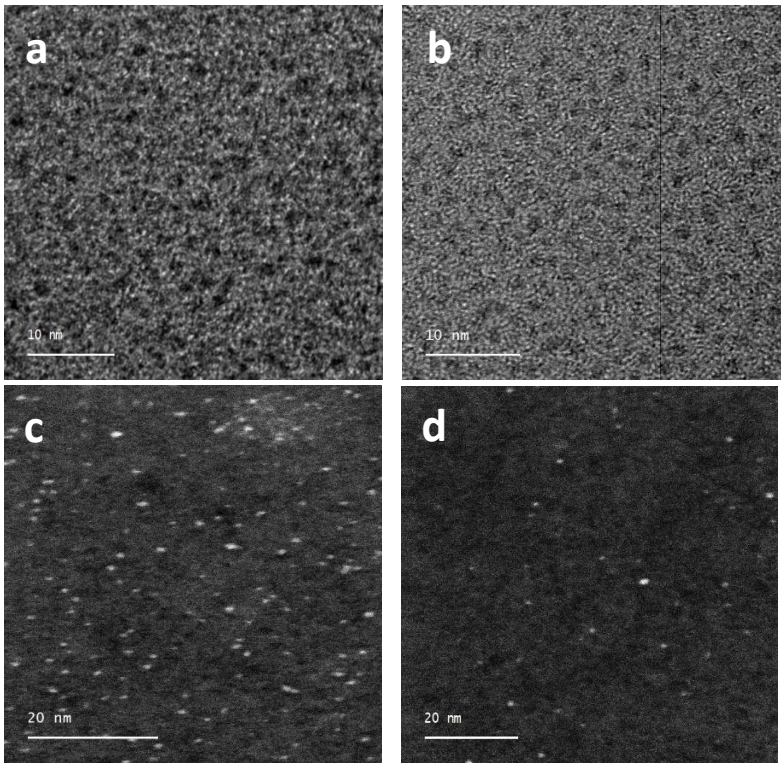


**Figure S9**: TEM images of (a) [$Au_{11}$:GSH] and (b) [$Au_{11}$:2-PET]. HAADF-STEM of (c) $Au_{11}(PPh_3)_7Br_3$; and (d) $Au_{25}(SC_2H_4Ph)_{18}^-$.

**Full range PM-IRRAS spectrum of [$Au_{11}$:2-PET]**

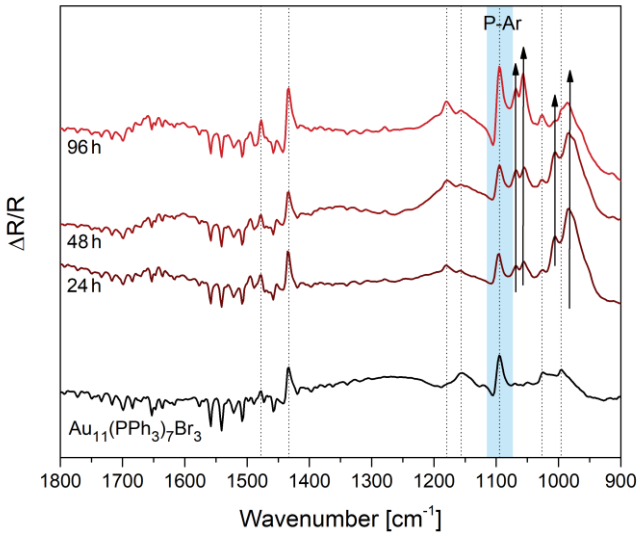


**Figure S10**: PM-IRRAS spectrum of the ligand exchange of supported $Au_{11}(PPh_3)_7Br_3$ with 2-PET. Bands evolving after reaction are indicated by arrows, bands from the initial $PPh_3$ ligands with dashed lines, and the colored area marks characteristic P-Ar vibrations of the $PPh_3$ ligands.

**MIR spectrum of 2-phenylethanethiol 2-PET**

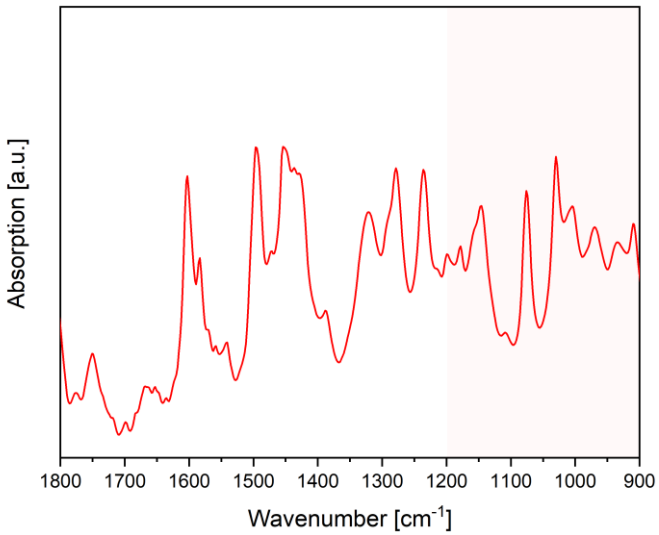


**Figure S11:** MIR spectrum of pure 2-PET. The pink area is the range of the PM-IRRAS spectrum of the [$Au_{11}$:2-PET] exchange shown in Figure 1b of the main paper.

**Ligand exchange of a $Au_{11}(PPh_3)_7Br_3$ dropcast on surface with GSH to product [$Au_{11}$:GSH]: Additional ATR-IR spectra**

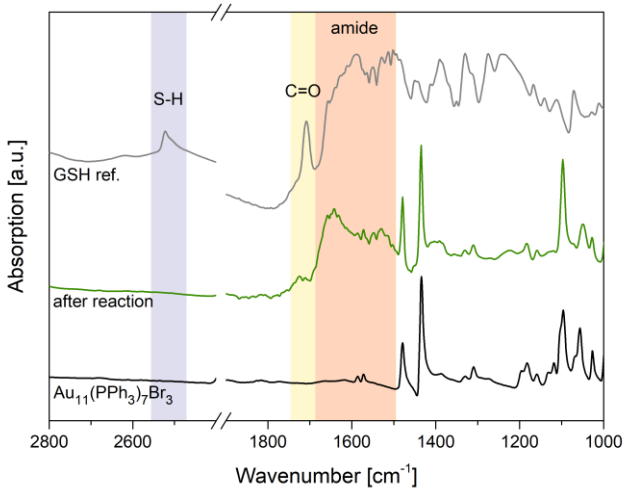


**Figure S12**: Comparison of the IR absorption of unreacted $Au_{11}(PPh_3)_7Br_3$ dropcast (bottom), the product [$Au_{11}$:GSH] after exchange (middle) and a GSH dropcast (top).

To exclude random absorption of the GSH ligands on the ZnSe crystal serving as support surface during the ATR experiment, a blank experiment was conducted. In that case, a solution of GSH in 8:2 $H_2O$:MeOH was flown through the ATR cell for a duration of 6h, thereby being in contact with the blank crystal surface. As can be seen in Figure S13, the difference in absorbance of the dry crystal surface before and after the blank experiment is negligible and can be related to changes in the ambient gas atmosphere (small differences in the $H_2O$ and $CO_2$ stretching vibration region). It is therefore assumed

that binding of the GSH ligands to the ZnSe support does not play a significant role within this experiment.

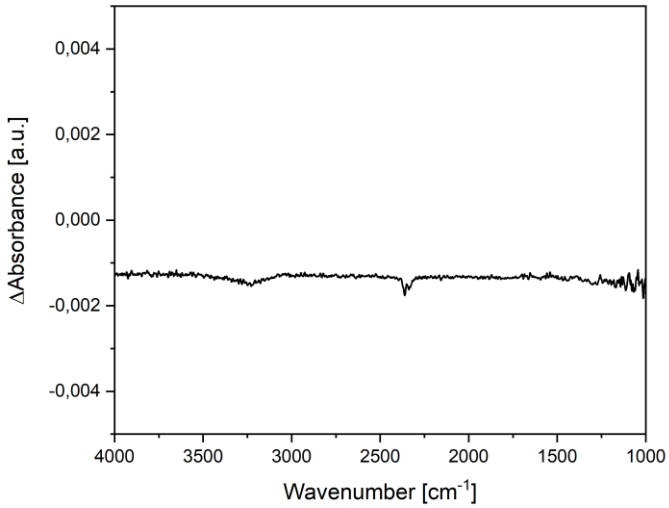


**Figure S13**: Differential Absorbance of the ZnSe crystal surface before and after flowing through a solution of GSH in $H_2O$:MeOH 8:2 for 6h.

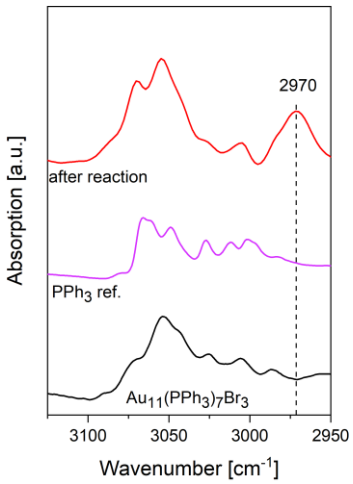


**Figure S14**: Comparison of the CH-stretching region of unreacted $Au_{11}(PPh_3)_7Br_3$ dropcast (black), the product [Au11:GSH] after exchange (red) and a $PPh_3$ dropcast (magenta).

**Ligand exchange of a $Au_{11}(PPh_3)_7Br_3$ dropcast on an $Al_2O_3$ surface with 2-PET to product [$Au_{11}$:2-PET]'**

The ligand exchange was conducted in the same way as described in the experimental section for product [$Au_{11}$:2-PET], with the only exception being the use of hexane instead of toluene as main solvent. This caused only minimal differences in the PM-IRRAS and MALDI-MS spectra, as well as in the TEM images, as comparison of Figure S15 with the corresponding data of [$Au_{11}$:2-PET] (see main part of the publication) shows. It is therefore concluded that the emerging products are of similar nature.

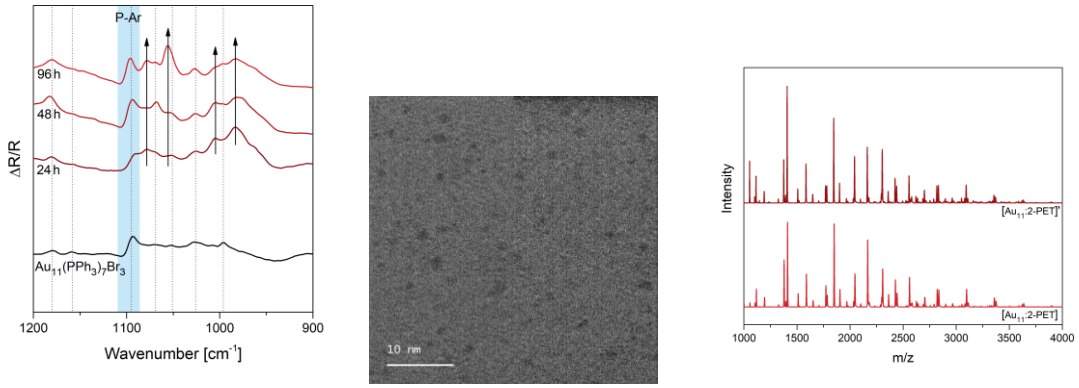


**Figure S15**: PM-IRRAS spectra of the ligand exchange of $Au_{11}(PPh_3)_7Br_3$ in hexane/$CHCl_3$ with 2-PET to [$Au_{11}$:2-PET]' (left), TEM image of [$Au_{11}$:2-PET]' (middle), MALDI-MS spectrum of [$Au_{11}$:2-PET]' and [$Au_{11}$:2-PET] (right)

**Additional photoluminescence spectra**

Photoluminescence spectra were recorded for the unreacted $Au_{11}(PPh)_3Br_3$ and the exchange products of the ligand exchange with GSH and 2-PET, $Au_{25}(SG)_{18}$ and $[Au_{25}(PPh_3)_{10}(2\text{-PET})_5Br_2]^{2+}$, using excitation at 400 nm (Figure S16). Due to instrumental limitations, the emission spectra could only be recorded up to 850 nm. As seen in Figure S16, $Au_{11}(PPh)_3Br_3$ did not exhibit any photoluminescence in the recorded energy region, also when varying excitation energies. The emission spectrum of $Au_{25}(SG)_{18}$ showed a band with an onset at ≈620 nm, which is in agreement with recorded spectra[17, 18]. $[Au_{25}(PPh_3)_{10}(2\text{-PET})_5Br_2]^{2+}$ also showed photoluminescence activity, exhibiting an emission band with a maximum >850 nm, again resembling published spectra[19].

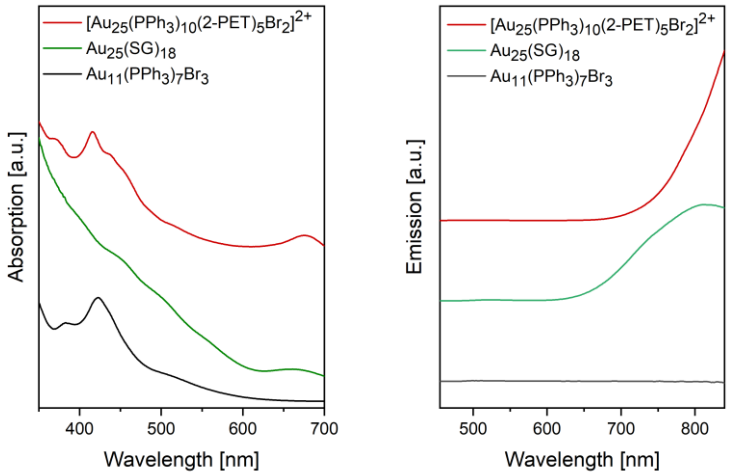


**Figure S16:** Absorption (left) and emission (right) spectra of the unreacted $Au_{11}(PPh)_3Br_3$ clusters and the products of the ligand exchange products in solution, $Au_{25}(SG)_{18}$ and $[Au_{25}(PPh_3)_{10}(2\text{-PET})_5Br_2]^{2+}$. Spectra were recorded of cluster solutions in DCM ($Au_{11}(PPh)_3Br_3$ and $[Au_{25}(PPh_3)_{10}(2\text{-PET})_5Br_2]^{2+}$) or water ($Au_{25}(SG)_{18}$). Emission spectra were recorded with a fixed excitation at 400 nm. Spectra were normalized and offset for clarity.

Spectral data of the as-synthesized F-GSH were also obtained (Figure S17). The fluorescein labeled thiol showed prominent fluorescence above 500 nm.

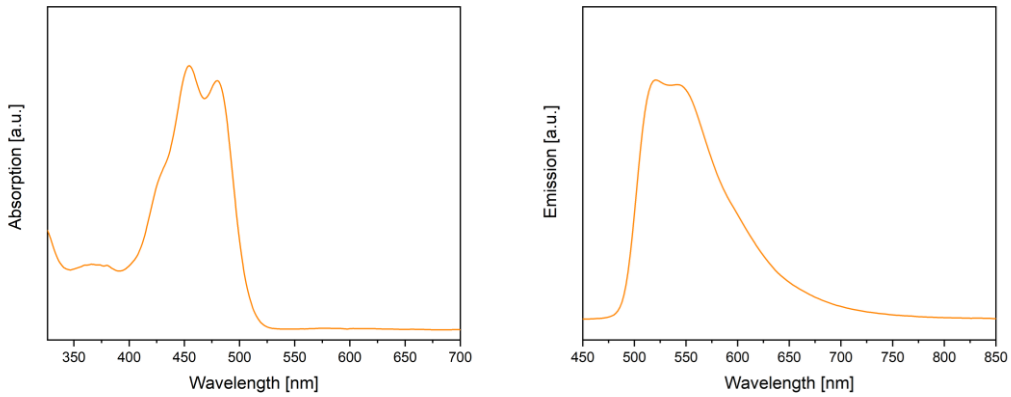


**Figure S17:** Absorption (left) and emission (right) spectrum of F-GSH, both measured as solution in methanol. The emission spectrum was recorded with a fixed excitation at 400 nm (the same as for the other dissolved analytes).

Photoluminescence spectra were also recorded of the products of the ligand exchange with $Au_{11}$ on an alumina surface, [$Au_{11}$:GSH] and [$Au_{11}$:2-PET]. The spectra were obtained as solid-state photoluminescence spectrum. Due to instrumental limitations, the emission spectra could only be recorded up to 700 nm. Excitation at both 400 and 450 nm was tested, however, no major influence on the observed emission spectra was found. Figure S18 shows the emission spectra of the products in comparison to the spectrum of the exchange product with the fluorescein tagged GSH, [$Au_{11}$:F-GSH]. As can be seen, the exchange with the F-GSH ligand induces fluorescence to the previously inactive $Au_{11}$ clusters, whereas exchange with GSH and 2-PET does not evoke photoluminescence.

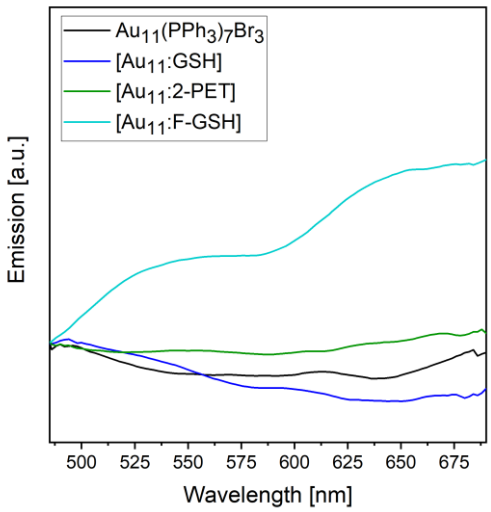


**Figure S18:** Emission spectra of unreacted $Au_{11}$, [$Au_{11}$:F-GSH], [$Au_{11}$:GSH] and [$Au_{11}$:2-PET]. Spectra were obtained in solid state (clusters dropcasts on a planar alumina surface) with fixed excitation at 450 nm.

## References


1. L. C. McKenzie, T. O. Zaikova and J. E. Hutchison, *J. Am. Chem. Soc.*, 2014, **136**, 13426-13435.
2. A. Shivhare, S. J. Ambrose, H. Zhang, R. W. Purves and R. W. J. Scott, *Chem. Commun.*, 2013, **49**, 276-278.
3. C. Liu, H. Abroshan, C. Yan, G. Li and M. Haruta, *ACS Catal.*, 2016, **6**, 92-99.
4. W. W. Weare, S. M. Reed, M. G. Warner and J. E. Hutchison, *J. Am. Chem. Soc.*, 2000, **122**, 12890-12891.
5. Z. Wu and R. Jin, *Chem. - Eur. J.*, 2013, **19**, 12259-12263.
6. L. M. Landino, C. M. Brown, C. A. Edson, L. J. Gilbert, N. Grega-Larson, A. J. Wirth and K. C. Lane, *Anal. Biochem.*, 2010, **402**, 102-104.
7. X. Kang, Y. Song, H. Deng, J. Zhang, B. Liu, C. Pan and M. Zhu, *RSC Adv.*, 2015, **5**, 66879-66885.
8. G. H. Woehrle, M. G. Warner and J. E. Hutchison, *J. Phys. Chem. B*, 2002, **106**, 9979-9981.
9. A. Das, T. Li, K. Nobusada, Q. Zeng, N. L. Rosi and R. Jin, *J. Am. Chem. Soc.*, 2012, **134**, 20286-20289.
10. Y. Shichibu, Y. Negishi, T. Watanabe, N. K. Chaki, H. Kawaguchi and T. Tsukuda, *J. Phys. Chem. C*, 2007, **111**, 7845-7847.
11. G. H. Woehrle, L. O. Brown and J. E. Hutchison, *J. Am. Chem. Soc.*, 2005, **127**, 2172-2183.
12. Y. Negishi, K. Nobusada and T. Tsukuda, *J. Am. Chem. Soc.*, 2005, **127**, 5261-5270.
13. K. Kimura, N. Sugimoto, S. Sato, H. Yao, Y. Negishi and T. Tsukuda, *J. Phys. Chem. C*, 2009, **113**, 14076-14082.
14. W. Nischkauer, F. Vanhaecke and A. Limbeck, *Anal. Bioanal. Chem.*, 2016, **408**, 5671-5676.
15. P. Pertl, M. S. Seifner, C. Herzig, A. Limbeck, M. Sistani, A. Lugstein and S. Barth, *Chemical Monthly*, 2018, **149**, 1315-1320.
16. Y. Liu, H. Tsunoyama, T. Akita and T. Tsukuda, *J. Phys. Chem. C*, 2009, **113**, 13457-13461.
17. M. Wang, Z. Wu, J. Yang, G. Wang, H. Wang and W. Cai, *Nanoscale*, 2012, **4**, 4087-4090.
18. Z. Wu, M. Wang, J. Yang, X. Zheng, W. Cai, G. Meng, H. Qian, H. Wang and R. Jin, *Small*, 2012, **8**, 2028-2035.
19. M. Zhou, J. Zhong, S. Wang, Q. Guo, M. Zhu, Y. Pei and A. Xia, *J. Phys. Chem. C*, 2015, **119**, 18790-18797.